Overestimation and Underestimation Biases in Photon Mapping with Non-Constant Kernels

Rubén Jesus García Hernández, Carlos Ureña, Jordi Poch, and Mateu Sbert

Abstract—This paper presents an analysis of the overestimation bias in common used filtering kernels in the context of photon mapping density estimation. We use the joint distribution of order statistics to calculate the expected value of the estimators of irradiance, and show that the estimator provided by the cone filter is not consistent unless the slope is one (yielding the triangular kernel), and that the Epanechnikov and Silverman kernels are consistent. The Gaussian filter has two different estimation biases: the original normalization constant α underestimates radiance by 46.9 percent, and the use of the kth nearest photon reduces this underestimation slightly. We also show that a new normalization constant for the Gaussian filter together with discarding the contribution of the kth nearest photon in the Gaussian and cone filter estimators produces new, consistent estimators. The specialized differential filter also benefits from the new estimate.

Index Terms—Kernel density estimation, order statistics, photon mapping

1 Introduction

Physical simulation of photon trajectories and their interaction with the objects in a scene provides an easy to understand means to generate realistic images. One very popular technique in this spirit is Photon mapping [1]. The technique has many variants, and can calculate efficiently many interesting effects. The core of the algorithm estimates irradiance at a given point by finding the k nearest photon impacts, adding their flux and dividing by the area of the smallest disc containing the k photons.

A weight depending on the distance to the point where radiance is being estimated is often used to provide smoothing. This avoids artifacts when the number of photons is small. The weight function is called a kernel. If no weights are used, the result is equivalent to using a constant kernel. This procedure is essentially a kernel density estimation technique [2].

In García et al. [3] it was shown that the photon mapping algorithm with constant kernel should discard the contribution of the kth nearest photon in order to avoid an overestimation bias. This result is a consequence of the correct k nearest neighbour estimate (introduced by Loftsgaarden [4] in the Statistics field). The result is also known in the Pattern Recognition field [5].

However, in the Photon Mapping literature, most approaches use k photons. Some implementations have used $k - 0.5$ when all photons carry the same flux (Dr. Per Christensen, private communication, 2012). Others have used the mean distance between the kth and $(k-1)$th photons (Dr. Reinhard Klein, private communication, 2013). Progressive photon mapping [6], [7] describes an asymptotically unbiased algorithm.

In the discussion following the exposition of García et al. [8], there was a general request to extend the framework and provide some use cases and examples detailing how to study more complex photon mapping variations. In this paper, we extend the framework by using the joint distribution of order statistics, in order to take into account non-constant kernels, and show a theoretical and empirical study of commonly used filtering kernels in photon mapping.

This extended framework opens the door to the study of a wide variety of photon mapping variants which use different strategies to weight the samples (some initial directions are described as future work). The biases detected and the means discovered to eliminate them will allow the development of more accurate algorithms. Additionally, the theoretical characterization of these algorithms will allow their use in Predictive Rendering [9] (creating formal guarantees on error in the final images generated).

Our results indicate that when the kernel is normalized and assigns weight 0 to the kth nearest photon, the estimator is consistent. Otherwise, the estimator is biased. This bias may be either the overestimation bias shown in García et al. [3], or an underestimation bias, depending on the parameters of the algorithm. We also show that discarding the kth nearest photon makes the studied estimators consistent (the Gaussian filter commonly used in photon mapping has an incorrect normalization constant creating an underestimation bias of up to 46.9 percent).

Section 2 describes photon mapping and variants using filtering kernels. Then Section 3 describes in detail our theoretical study, with Section 3.1 studying photon tracing and final gathering, Section 3.2 introducing order statistics, and Section 3.3 applying order statistics to photon mapping density estimation for a general kernel. Then Sections 3.4 to 3.8 study the expected value of the

- *R. J. García Hernández, J. Poch, and M. Sbert are with the Department of Informatics and Applied Mathematics, University of Girona, Spain. E-mail: rubengarciahernandez@gmail.com, {jordi.poch, mateu}@ima.udg.edu.*
- *C. Ureña is with the Department of Languages and Computer Systems of the University of Granada, Spain. E-mail: curena@ugr.es.*

Manuscript received 30 Apr. 2013; revised 27 Jan. 2014; accepted 14 Mar. 2014. Date of publication 31 Mar. 2014; date of current version 27 Aug. 2014. Recommended for acceptance by G. Drettakis.
For information on obtaining reprints of this article, please send e-mail to: reprints@ieee.org, and reference the Digital Object Identifier below.
Digital Object Identifier no. 10.1109/TVCG.2014.2314665

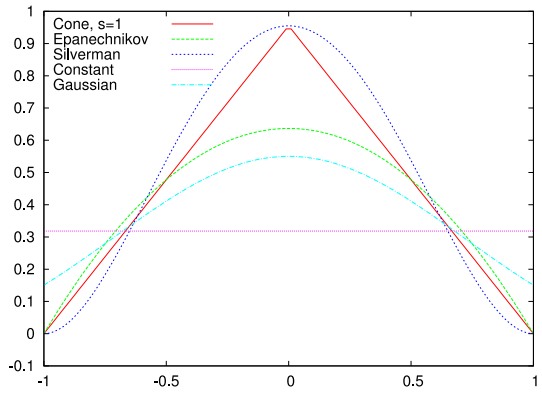

Fig. 1. Density estimation kernels.

irradiance estimate for the cone filter [1], the Epanechnikov kernel [10], the Silverman kernel [11], the Gaussian kernel and the specialized differential filter, respectively. Section 3.9 contains a study of progressive photon mapping. Section 4 contains an empirical study of the kernels, with Section 4.1 using a directional light source and Section 4.2 a point light source. Finally Section 5 provides the conclusions.

2 Photon Mapping with Filtering Kernel

In this section, we will detail the photon mapping algorithm in some detail, along with the known sources of bias. The photon mapping algorithm includes several computation steps:

Photon tracing. Photons are traced from the light sources and reflected or absorbed upon interaction with the scene. Each impact is recorded in a kd-tree data structure.

Ray tracing (from the eye). Rays are traced from the eye into the scene. On the intersection point with a surface of the scene, either a photon map query is performed, yielding the estimated radiance at the point, or a number of secondary rays are raytraced (*final gather*), and the photon mapping queries from the secondary impacts are integrated to yield an improved radiance estimate. In both cases density estimation (see below) must be done.

Density estimation (photon map query). For a given point on a surface, the flux of the k nearest impacts recorded in the kd-tree is added, and divided by the area of a disc with the radius equal to the distance between the point and the kth impact.

The contribution of the k nearest photons is commonly weighted by a filtering kernel. Jensen recommended a cone filter [1]; the Epanechnikov kernel was used by Walter [10] and the Silverman kernel by Shirley [11]. The Gaussian kernel and the specialized differential filter have also been used, along with other filtering strategies [12].

Fig. 1 shows the weight given by the kernels studied in this article to the photon impacts located near the point of interest (at the origin). The distance of the kth nearest impact is 1 in the graph.

The photon mapping algorithm is known to be biased, and the following biases have been described [12], [13], [3]:

TABLE 1
Symbols Used in this Article

Combinatorials in order statistics	
$\mathcal{C} = \frac{n!}{(k-1)!(n-k)!}$	Constant in univariate case.
$\mathcal{C}_J = \frac{n!}{(i-1)!(k-i-1)!(n-k)!}$	Joint distribution constant.
$\mathcal{C}_K = 2\mathcal{C}_J r_k \left[1 - r_k^2\right]^{n-k}$	Auxiliary combinatorial.

Photon mapping parameters	
P	Point where a photon map query is done.
n	Number of photon impacts.
k	Number of photons sought in a Photon Maps query.
r_k	Distance of the kth nearest photon in a query. r_k follows the distribution $f_{X_{(k)}}$.
ϕ	Flux.
s	Slope of the cone filter.
Distribution functions	
g	Area density of photon impacts.
f	Area density at a given distance of the photon map query.
F	Accumulated distribution of f.
$f_{X_{(k)}}$	kth order statistics of f.
$f_{X_{(i,k)}}$	Joint distribution of the ith and kth order statistics of f.
Irradiance and expected values	
$K_{r_k}(r_i)$	Filtering kernel.
I	Irradiance.
$\widehat{I}$	Photon mapping irradiance estimate.
$\widehat{I_i^*}$, $\widehat{I_k^*}$	Estimate of the contribution of the ith (respectively kth) nearest photon to $\widehat{I}$.
E[]	Expected value.
E_{k-1}	$\sum_{i=1}^{k-1} E[\widehat{I_i^*}]$.

Proximity. The estimate converges to the weighted mean irradiance in a neighbourhood of the point.

Boundary. The estimate is too dark near borders, since the area contains an unreachable zone where no surface exists.

Topological. This bias appears if surfaces are not locally planar.

Overestimation. Adding the contribution of the kth nearest impact produces an overestimation bias.

3 Theoretical Study of Convergence

We will present here the basis for the study of filtering kernels in photon mapping. The symbols used repeatedly in the paper can be seen in Table 1.

3.1 Photon Tracing, BRDFs and Final Gathering

The following sections describe how biases in the density estimation phase of photon mapping (studied in detail in Sections 3.2 to 3.8) is transferred to the final radiance estimate by the other phases of the algorithm.

3.1.1 Photon Tracing

Tracing the photons from the light sources and reflecting and absorbing them according to the BRDF will produce a probabilistic distribution of photon flux proportional to irradiance.

There are many causes of photons with different flux values. In general the situation appears when the transition probability function between states in the Markov chain is not proportional to the kernel of the integral equation governing the behaviour of the photons. Survival probabilities not proportional to albedo or output direction not proportional to the BRDF are examples.

The system can be modelled by a probabilistic distribution function $\tilde{g}(P,\phi)$ defined on the domain $S \times \mathbb{R}$, where S is the set of all surface points in the scene, and $\phi \in \mathbb{R}$ is the flux. For all points P in S, we have (similarly to García et al. [3] where g is the photon density function)

$$\int_0^\infty \phi\tilde{g}(P,\phi)\mathrm{d}\phi = \frac{I(P)}{n}, \tag{1}$$

(that is, changes in photon density are offset by changes in photon flux, so that irradiance is conserved; this is a consequence of the photon tracing method being unbiased). The estimate which takes into account the flux of the photons is (constant kernel case)

$$\widehat{I}(\langle r_1,\phi_1\rangle,\ldots,\langle r_k,\phi_k\rangle) = \frac{\sum_{i=1}^k \phi_i}{\pi r_k^2} = \sum_{i=1}^k \frac{\phi_i}{\pi r_k^2}, \tag{2}$$

where ϕ_i is the flux of the ith nearest photon, and $r_1,\ldots,r_k$ are the distances of the first, $\ldots$, kth nearest photons.

These equations can be used to extend the study of the constant kernel photon mapping estimate [3] and the kernels in the following sections for the case in which photons have different flux (expected values become a double or triple integral, and equations (1) and (2) can be used to show that the photon map overestimation bias is preserved).

3.1.2 Final Gathering

Now we focus on how the bias is conserved in the final gathering phase. To calculate the estimated radiance at the point of interest P, the BRDF is used to measure the contribution of the incoming photons reflected towards the observer. Three cases can be distinguished:

Diffuse surfaces. The contribution of the nearest photons are added and the result divided by the area of the disc of radius r_k. The radiance is calculated by multiplying this by the diffuse coefficient, which is a constant. It is easy to see that the overestimation of irradiance produces an equivalent overestimation of radiance.

Glossy surfaces. The incoming direction of each photon is also taken into account, and the BRDF indicates the fraction of flux leaving towards the observer. The contribution of all photons are added after the reflection by the BRDF. Again, overestimation of irradiance produces an equivalent overestimation of radiance.

Final gathering. That is, raytrace of a number of rays from P (averaging the values of the photon maps queries at the secondary impact points). Each of the secondary photon map queries will have an overestimation of irradiance, which produces an overestimation of radiance, as the previous two points indicate. Averaging these estimates again produces the equivalent overestimation of radiance at P.

3.2 Order Statistics

Order statistics deal with the probability distribution of elements in ordered lists. When we sample a continuous random phenomenon which has a probability distribution f, the result is a list of real values $[x_1,\ldots,x_n]$. After ordering this list, we obtain $[x_{(1)},\ldots,x_{(n)}]$, where $x_{(1)}$ is the minimum value, and $x_{(n)}$ the maximum. Even though all x_k have the same probability density function f, the probability distribution of the $x_{(k)}$ depends on f, n and k, by the following formula [14], [3]:

$$f_{X_{(k)}}(x) = \mathcal{C}(F(x))^{k-1}(1-F(x))^{n-k}f(x), \tag{3}$$

where F is the cumulative distribution function corresponding to f and

$$\mathcal{C} = \frac{n!}{(k-1)!(n-k)!}. \tag{4}$$

The joint distribution of two random variables gives the probability density of events defined in terms of the two variables. The joint distribution of two order statistics has the following formula for $x < y$ [14]:

$$f_{X_{(i,k)}}(x,y) = \mathcal{C}_J[F(x)]^{i-1}f(x)[\mathcal{G}(x,y)]^{k-i-1}f(y)[\mathcal{F}(y)]^{n-k} \tag{5}$$

with

$$\mathcal{C}_J = \frac{n!}{(i-1)!(k-i-1)!(n-k)!} \tag{6}$$

and

$$\mathcal{F}(x) = 1-F(x) \qquad \mathcal{G}(x,y) = F(y)-F(x). \tag{7}$$

For values of x and y fulfilling $x \geq y$, $f_{X_{(i,k)}}(x,y) = 0$.

We will use $f_{X_{(k)}}(x)$ to study the contribution of the kth nearest photon and $f_{X_{(i,k)}}$ to study the contribution of the $k-1$ nearest photons in photon mapping with filtering kernels in the following sections.

3.3 Application of Order Statistics to Photon Mapping

We will calculate the expected value of the Photon Maps estimators for a unit disc with uniform irradiance. We assume all photons carry the same flux $\phi = \frac{\pi I(P)}{n}$. The location of impacts has a constant distribution function

$$g(P) = \frac{1}{\pi}, \tag{8}$$

with P being a point in the unit disc. The probability density of photons at distance r and the cummulative distributions are

$$f(r) = 2r \qquad F(r) = r^2. \tag{9}$$

The distribution of the kth order statistic (the distance of the impact sought by Photon Maps) is

$$f_{X_{(k)}}(r) = \mathcal{C}(F(r))^{k-1}(1-F(r))^{n-k} f(r). \tag{10}$$

Substituting, we get

$$f_{X_{(k)}}(r) = \mathcal{C}2r^{2k-1}\left(1-r^2\right)^{n-k}. \tag{11}$$

The joint distribution is (equation (5))

$$\begin{aligned} &f_{X_{(i,k)}}(r_i, r_k) \\ &\quad = \mathcal{C}_J[F(r_i)]^{i-1} f(r_i)[\mathcal{G}(r_i, r_k)]^{k-i-1} f(r_k)[\mathcal{F}(r_k)]^{n-k} \\ &\quad = \mathcal{C}_K 2r_i^{2i-1}\left[r_k^2 - r_i^2\right]^{k-i-1} \end{aligned} \tag{12}$$

with

$$\mathcal{G}(r_i, r_k) = F(r_k) - F(r_i) = r_k^2 - r_i^2, \tag{13}$$

$$\mathcal{F}(r_k) = 1 - F(r_k) = 1 - r_k \tag{14}$$

and we define $\mathcal{C}_K$ as

$$\mathcal{C}_K = 2\mathcal{C}_J r_k\left[1 - r_k^2\right]^{n-k}. \tag{15}$$

This joint distribution is needed to calculate the contribution of the $k-1$ closest impacts when using a non-constant kernel, because the irradiance estimate uses the location of impacts i and k in the evaluation of the kernel.

In the following sections, we will use $K_{r_k}(r_i)$ to denote the different kernels, and will use $\widehat{I}$ to denote the irradiance estimate of the different methods. The contribution of the specific photons are denoted $\widehat{I}_i^*$ and $\widehat{I}_k^*$, where the star indicates the fact that this is not an irradiance estimate, but an auxiliar value. We used the non-standard $I()$ for irradiance in order to distinguish it from the notation for expected value $E[]$, following García et al. [3].

The following sections contain studies of the Cone filter (Section 3.4), the 2D Epanechnikov kernel (Section 3.5), the Silverman kernel (Section 3.6), the Gaussian filter (Section 3.7), the specialized differential filter (Section 3.8) and a study of progressive photon mapping (Section 3.9).

3.4 Cone Filter

The cone filter was used by Jensen [1]. Let us call s the slope of the cone filter

$$K_{r_k}(r_i) = \frac{1 - \frac{r_i}{sr_k}}{\pi r_k^2\left(1 - \frac{2}{3s}\right)} \tag{16}$$

If $s = 1$, the weight of the kth nearest photon is 0:

$$K_{r_k}(r_k) = \frac{1 - \frac{r_k}{r_k}}{\pi r_k^2\left(1 - \frac{2}{3}\right)} = 0 \tag{17}$$

The estimator is

$$\widehat{I}(r_1, \ldots, r_k) = \sum_{i=1}^{k} K_{r_k}(r_i)\phi. \tag{18}$$

We will study the contribution of each photon separately (we denote $\widehat{I}_i^*$ the contribution of the ith nearest photon, and $\widehat{I}_k^*$ that of the kth)

$$\widehat{I}_i^*(r_i, r_k) = K_{r_k}(r_i)\phi = \frac{1 - \frac{r_i}{sr_k}}{\pi r_k^2\left(1 - \frac{2}{3s}\right)}\phi \tag{19}$$

$$\widehat{I}_k^*(r_k) = K_{r_k}(r_k)\phi = \frac{1 - \frac{1}{s}}{\pi r_k^2\left(1 - \frac{2}{3s}\right)}\phi \tag{20}$$

3.4.1 Contribution of Impacts $i < k$

The expected value of the estimators of the contribution of the ith nearest photon is

$$\begin{aligned} E[\widehat{I}_i^*] &= \int_0^1 \int_0^{r_k} \widehat{I}_i^*(r_i, r_k) f_{X_{(i,k)}}(r_i, r_k)\mathrm{d}r_i\mathrm{d}r_k \\ &= \int_0^1 \int_0^{r_k} \frac{1 - \frac{r_i}{sr_k}}{\pi r_k^2\left(1 - \frac{2}{3s}\right)}\phi\mathcal{C}_K 2r_i^{2i-1}\left[r_k^2 - r_i^2\right]^{k-i-1}\mathrm{d}r_i\mathrm{d}r_k \\ &= \frac{\phi}{\pi\left(1 - \frac{2}{3s}\right)} n\left(\frac{1}{k-1} - \frac{\Gamma\left(i+\frac{1}{2}\right)\Gamma(k-1)}{s\,\Gamma(i)\Gamma\left(k+\frac{1}{2}\right)}\right), \end{aligned} \tag{21}$$

(see Appendix A, which can be found on the Computer Society Digital Library at http://doi.ieeecomputersociety.org/10.1109/TVCG.2014.2314665, for the proofs of the results in this and the following section). We will now add the contribution of the $k-1$ nearest impacts (we denote this sum E_{k-1}):

$$E_{k-1} = \sum_{i=1}^{k-1} E\left[\widehat{I}_i^*\right] = I(P). \tag{22}$$

3.4.2 Contribution of Impact k

We calculate the expected value of the contribution of impact k as

$$\begin{aligned} E[\widehat{I}_k^*] &= \int_0^1 \widehat{I}_k^*(r_k) f_{X_{(k)}}(r_k)\mathrm{d}r_k \\ &= \int_0^1 \frac{1 - \frac{1}{s}}{\pi r_k^2\left(1 - \frac{2}{3s}\right)}\phi\mathcal{C}2r_k^{2k-1}\left(1 - r_k^2\right)^{n-k}\mathrm{d}r_k \\ &= \frac{(3s-3)I(P)}{(3s-2)(k-1)}. \end{aligned} \tag{23}$$

3.4.3 Expected Value of the Estimator

The expected value is

$$E[\widehat{I}] = E_{k-1} + E[\widehat{I}_k^*] = I(P) + \frac{(3s-3)I(P)}{(3s-2)(k-1)}. \tag{24}$$

Fig. 2 shows the relative bias for different values of the slope, for $k = 2$. We can see from equation (24) that the slope $s = 1$ (in which the contribution of the kth nearest impact is zero) creates no bias, while larger values overestimate radiance. Values of s between 0 and $2/3$ overestimate radiance as well, while values between $2/3$ and 1 underestimate radiance (in this case we should talk of underestimation bias).

The kernel cannot be evaluated in the case $s = 2/3$ due to a division by zero error. Additionally, it is easy to see that if the contribution of the kth nearest photon is discarded, an arbitrary slope (except $2/3$) can be chosen.

The bias for other values of k can be obtained by scaling the graph in Fig. 2 by $1/(k-1)$ (this is a consequence of equation (23)). Large values of k have a small bias, which may be hidden in the noise if s is not near $2/3$.

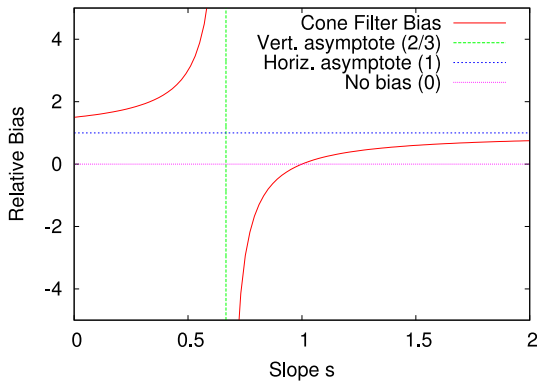

Fig. 2. Relative bias of photon mapping with a cone filter for a uniform distribution of photons, as a function of the slope s, for $k = 2$.

3.5 2D Epanechnikov Kernel

The 2D Epanechnikov kernel used by Walter [10] is

$$K_{r_k}(r_i) = \frac{2}{\pi r_k^2}\left[1 - \left(\frac{r_i}{r_k}\right)^2\right]. \tag{25}$$

The expected value of the estimator can be calculated similarly to the previous section. By construction, $K_{r_k}(r_k) = 0$, so we only need to study photons $i < k$.

The estimator, again, is

$$\widehat{I}(r_1, \ldots, r_k) = \sum_{i=1}^{k} K_{r_k}(r_i)\phi. \tag{26}$$

The expected value of the estimator is (see Appendix B, available in the online supplemental material)

$$\begin{aligned} E[\widehat{I}_i^*] &= \int_0^1 \int_0^{r_k} \widehat{I}_i^*(r_i, r_k) f_{X_{(i,k)}}(r_i, r_k) \mathrm{d}r_i \mathrm{d}r_k \\ &= \frac{2\phi}{\pi} \frac{(k-i)n}{(k-1)k}. \end{aligned} \tag{27}$$

The contribution of the $k-1$ nearest photons is

$$E_{k-1} = \sum_{i=1}^{k-1} E[\widehat{I}_i^*] = \sum_{i=1}^{k-1} \frac{2\phi}{\pi} \frac{(k-i)n}{(k-1)k} = \frac{2\phi}{\pi}\frac{n}{2} = \frac{\phi n}{\pi} = I(P) \tag{28}$$

We can see that the estimator is consistent.

3.6 Silverman Kernel

The Silverman kernel [15] is

$$K_{r_k}(r_i) = \frac{3}{\pi r_k^2}\left[1 - \left(\frac{r_i}{r_k}\right)^2\right]^2. \tag{29}$$

We can see that the contribution of the kth nearest photon is zero.

The estimator, as with previous sections, is (see Appendix C, available in the online supplemental material, for details)

$$\widehat{I}(r_1, \ldots, r_k) = \sum_{i=1}^{k} K_{r_k}(r_i)\phi. \tag{30}$$

The expected value of the estimator of the contribution of the ith nearest photon is

$$\begin{aligned} E[\widehat{I}_i^*] &= \int_0^1 \int_0^{r_k} \widehat{I}_i^*(r_i, r_k) f_{X_{(i,k)}}(r_i, r_k) \mathrm{d}r_i \mathrm{d}r_k \\ &= \frac{3\phi(k-i+1)(k-i)n}{\pi(k^2-1)k}. \end{aligned} \tag{31}$$

The contribution of the $k-1$ nearest photons is

$$E_{k-1} = \sum_{i=1}^{k-1} E[\widehat{I}_i^*] = \sum_{i=1}^{k-1} \frac{3\phi}{\pi} \frac{(k-i+1)(k-i)n}{(k^2-1)k} = I(P). \tag{32}$$

Since the contribution of the k nearest photon is zero, the estimator is consistent as well.

3.7 Gaussian Filter

The Gaussian filter described in Jensen's PhD [16] is

$$K_{r_k}(r_i) = \frac{1}{\pi r_k^2}\alpha\left[1 - \frac{1 - e^{-\beta\frac{r_i^2}{2r_k^2}}}{1 - e^{-\beta}}\right], \tag{33}$$

where $\alpha = 0.918$ and $\beta = 1.953$ following Pavicik [17]. Observe that in [18] and [19] the factor $1/\pi r_k^2$ is missing. Another consideration worth noting is that the normalization constant α in Pavicic [17] applies to the unit square over which Pavicik is smoothing (a pixel). Since the kernel support in Photon Mapping is the unit disk, the correct normalization constant is

$$\tilde{\alpha} = \frac{\beta(e^\beta - 1)}{2e^\beta - 2e^{\beta/2} - \beta}. \tag{34}$$

For the chosen $\beta = 1.953$, $\tilde{\alpha} = 1.728$ (see Appendix D, available in the online supplemental material, for the proofs of the results in this and the following sections).

Following previous sections, the estimator is

$$\widehat{I}(r_1, \ldots, r_k) = \sum_{i=1}^{k} K_{r_k}(r_i)\phi \tag{35}$$

3.7.1 *Contribution of Impacts $i < k$*

The estimator of the contribution of each photon $i < k$ to the radiance estimate is

$$\begin{aligned} E[\widehat{I}_i^*] &= \int_0^1 \int_0^{r_k} \widehat{I}_i^*(r_i, r_k) f_{X_{(i,k)}}(r_i, r_k) \mathrm{d}r_i \mathrm{d}r_k \\ &= \int_0^1 \int_0^{r_k} \frac{1}{\pi r_k^2}\tilde{\alpha}\left[1 - \frac{1 - e^{-\beta\frac{r_i^2}{2r_k^2}}}{1 - e^{-\beta}}\right] \phi \mathcal{C}_K 2 r_i^{2i-1}\left[r_k^2 - r_i^2\right]^{k-i-1} \mathrm{d}r_i \mathrm{d}r_k \\ &= \frac{\beta}{2e^\beta - 2e^{\beta/2} - \beta}\frac{\phi}{\pi}\frac{n\left(e^\beta {}_1F_1\left(i, k, -\frac{\beta}{2}\right) - 1\right)}{(k-1)}, \end{aligned} \tag{36}$$

where ${}_1F_1$ is the Kummer confluent hypergeometric function [20].

We will now add the contribution of the $k-1$ nearest impacts (we denote the expected value $E_{k-1} = \sum_{i=1}^{k-1} E[\widehat{I}_i^*]$):

$$E_{k-1} = \sum_{i=1}^{k-1} E[\widehat{I}_i^*] = I(P). \tag{37}$$

3.7.2 Contribution of Impact k

The evaluation of the kernel at the kth nearest photon is

$$K_{r_k}(r_k) = \frac{1}{\pi r_k^2}\tilde{\alpha}\left[1 - \frac{1 - e^{\frac{-\beta}{2}}}{1 - e^{-\beta}}\right] = \frac{\tilde{\alpha}}{\pi r_k^2}\frac{1}{1 + e^{\beta/2}}. \tag{38}$$

We calculate the expected value of the contribution of impact k as

$$\begin{aligned} E[\widehat{I}_k^*] &= \int_0^1 \widehat{I}_k^*(r_k) f_{X_{(k)}}(r_k)\mathrm{d}r_k \\ &= \int_0^1 \frac{\tilde{\alpha}}{\pi r_k^2}\frac{1}{1 + e^{\beta/2}}\phi\mathcal{C}2r_k^{2k-1}\left(1 - r_k^2\right)^{n-k}\mathrm{d}r_k \\ &= \frac{\beta(e^{\beta/2} - 1)}{(2e^{\beta} - 2e^{\beta/2} - \beta)}\frac{1}{k-1}I(P) \approx \frac{0.4728}{k-1}I(P). \end{aligned} \tag{39}$$

3.7.3 Expected Value of the Estimator

The expected value is

$$\begin{aligned} E[\widehat{I}] &= E_{k-1} + E[\widehat{I}_k^*] \\ &= \left(1 + \frac{\beta(e^{\beta/2} - 1)}{(2e^{\beta} - 2e^{\beta/2} - \beta)}\frac{1}{k-1}\right)I(P) \\ &\approx \left(1 + \frac{0.4728}{k-1}\right)I(P). \end{aligned} \tag{40}$$

The estimator which uses the original $\alpha = 0.918$ has an additional underestimation bias of $(1 - \alpha/\tilde{\alpha}) \approx 46.9\%$.

3.8 Specialized Differential Filter

The differential filter detects discontinuities in radiance by noticing that the changes in the estimate become monotonic near the edges. In this case, the algorithm will stop adding photons and use an estimate with fewer photons. Formally, we will use an estimate with $\tilde{k} \leq k$ photons, where we expect $\tilde{k}$ not to cross discontinuities.

The overestimation shown in [3] regarding the constant kernel applies also to this filter, with the classic estimate overestimating radiance by $\tilde{k}/(\tilde{k} - 1)$. Although the use of $\tilde{k}$ produces an increase of overestimation bias, the avoidance of the boundary crossing reduces the proximity and boundary biases. For discontinuities in radiance larger than $1/k$, we expect a global decrease in bias when using this filter with the original estimate.

The use of the corrected estimate will remove overestimation bias completely with no adverse effects, retaining the reduction in proximity and boundary biases.

3.9 Progressive Photon Mapping

Progressive photon mapping is an approach to transform photon mapping into an asymptotically unbiased algorithm. Hachisuka et al. [6] shows (for photon mapping with constant kernel) that as the number of photons shot n tends to infinity, and the number of photons k in a query also tends to infinity, but slower, then r_k tends to zero and the algorithm is asymptotically unbiased. The result is extended to general kernels having unit integral and a vanishing first moment by Knaus and Zwicker [7].

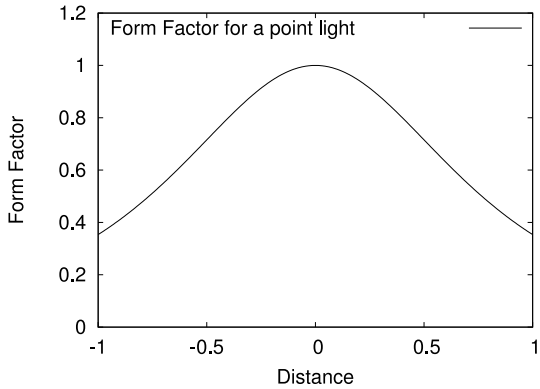

Fig. 3. Form factor for an omnidirectional light source located above the centre of a disc, at one unit of distance.

However, the algorithm they develop does not make use of this fact. Instead, a first photon mapping execution is used to derive a first $r_{(1,k)}$, in stage 1, and further photon mapping executions use a fixed radius which is calculated deterministically from this $r_{(1,k)}$. The final image is the average of the images generated in stages $1 \ldots S$. In stage $i + 1$, the radius $r_{(i+1,k)}$ follows:

$$\frac{r_{(i+1,k)}^2}{r_{(i,k)}^2} = \frac{i + \alpha}{i + 1} \tag{41}$$

in the standard case and

$$\frac{r_{(i+1,k)}^3}{r_{(i,k)}^3} = \frac{i + \alpha}{i + 1}, \tag{42}$$

in the volumetric case. α, satisfying $0 < \alpha < 1$, controls the how quickly variance increases and bias decreases in each iteration.

Since the radius is fixed, and independent of the order statistics of the distance of the kth nearest photon in that execution, progressive photon mapping reverts from k-nearest neighbour density estimation to basic density estimation.

Basic density estimation is not affected by the over- and under-estimation biases described in this paper, and therefore, the over-estimation bias present in the final image is $1/kS$ if a constant kernel is used. If other kernels are used, the results mentioned in the cone, gaussian and specialized differential filter Sections 3.4, 3.7 and 3.8 should also be divided by S to obtain the final over- and under-estimation bias. If the Epanechnikov or Silverman kernels were used, or if using a corrected photon mapping variant, the algorithm will have no overestimation bias.

4 Empirical Study

Fig. 1 contains the graph of the weighting of the photons for the different kernels. We can see that the cone filter with $s < 2/3$ produces higher weights for far away photons and has a negative weight for nearby ones, so it shouldn't be used. If $2/3 < s < 1$, the filter weights nearby photons more than far away photons, but distant photons have a negative weight, which also looks strange (discarding photons with negative weight will again overestimate radiance).

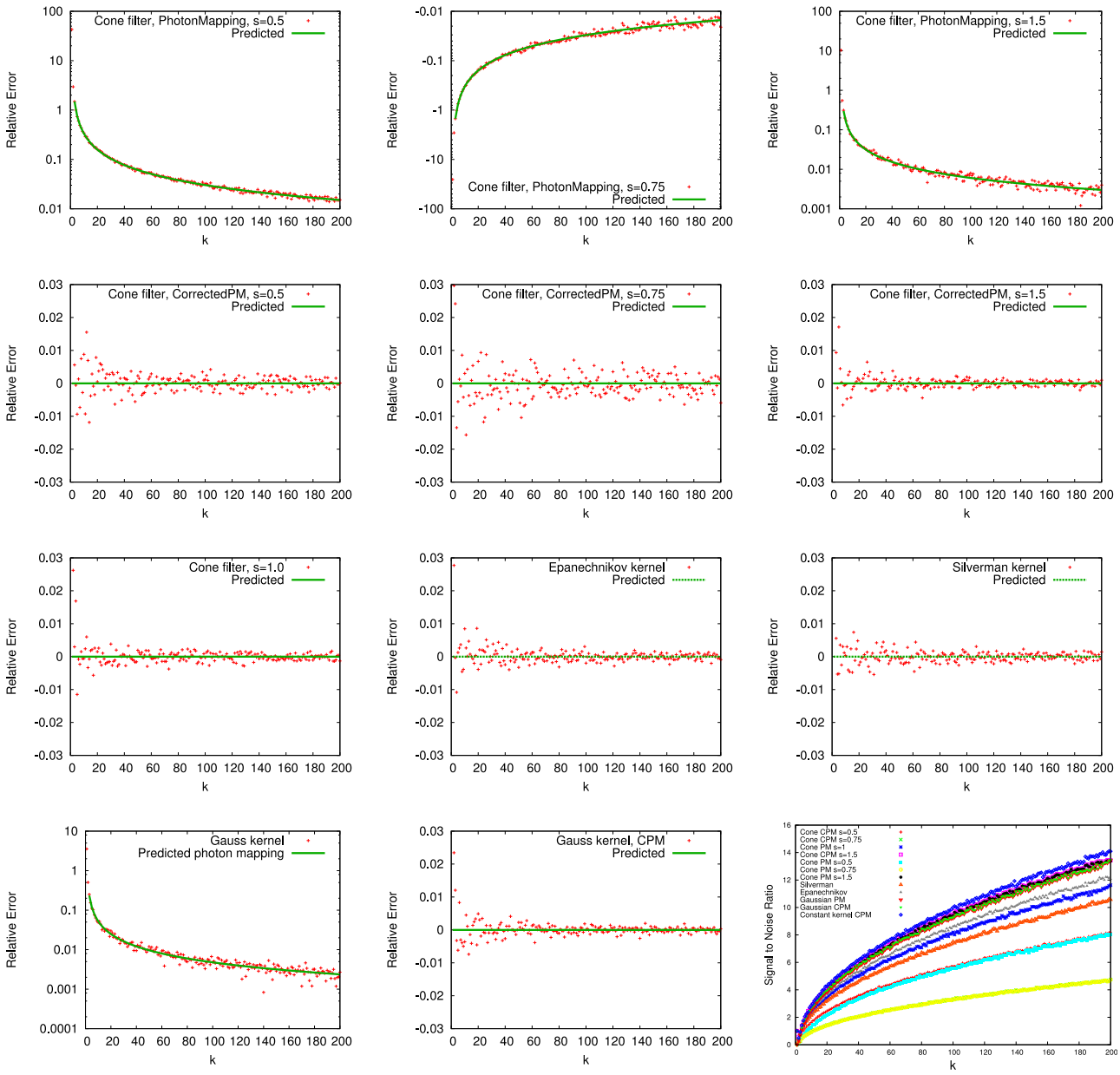

Fig. 4. Relative error of photon mapping (first row, logarithmic plot) and corrected photon mapping (second row, linear plot) with a cone filter using $s = 0.5$ (left), $s = 0.75$ (center), and $s = 1.5$ (right). Third row: Cone filter using $s = 1$ (left), Epanechnikov kernel (center) and Silverman kernel (right). Bottom row: Photon mapping (left) and corrected photon mapping (center) using a Gaussian filter. Right: signal to noise ratio of the different filters. Uniform distribution of photons as a function of k (in red); theoretical prediction of the error (in green). The (-1) bias with $k = 1$ for corrected photon mapping is not shown.

We will study the different kernels for two simple scenes: a planar disc illuminated by a directional light and the same planar disc illuminated by a point light source. The next two sections provide the details.

4.1 Empirical Study of a Directional Light

We have implemented in C++ a scene consisting of a planar unit disc illuminated by a directional light source, and calculated the photon mapping irradiance estimate for $n = 100{,}000$ and k ranging between 1 and 200, using the cone filter, the Epanechnikov kernel and the Silverman kernel. We have repeated the simulations ten thousand times to calculate an estimate of the convergence of the algorithm.

Fig. 2 shows that the bias of the cone filter estimate is a function of s, and that the possible values of s can be classified in four regions ($]$[denotes an open set):

$$s \in \left]0, \frac{2}{3}\right[s \in \left]\frac{2}{3}, 1\right[s = 1 \; s > 1. \tag{43}$$

We simulated the photon mapping irradiance estimate with a cone filter with slope parameters $s = 0.5$, $s = 0.75$, $s = 1$ and $s = 1.5$, to study these regions.

We will start by calculating the expected overestimation bias for $s = 0.5$, $s = 0.75$ and $s = 1.5$, since Section 3.4.3 shows that the bias is 0 for $s = 1$.

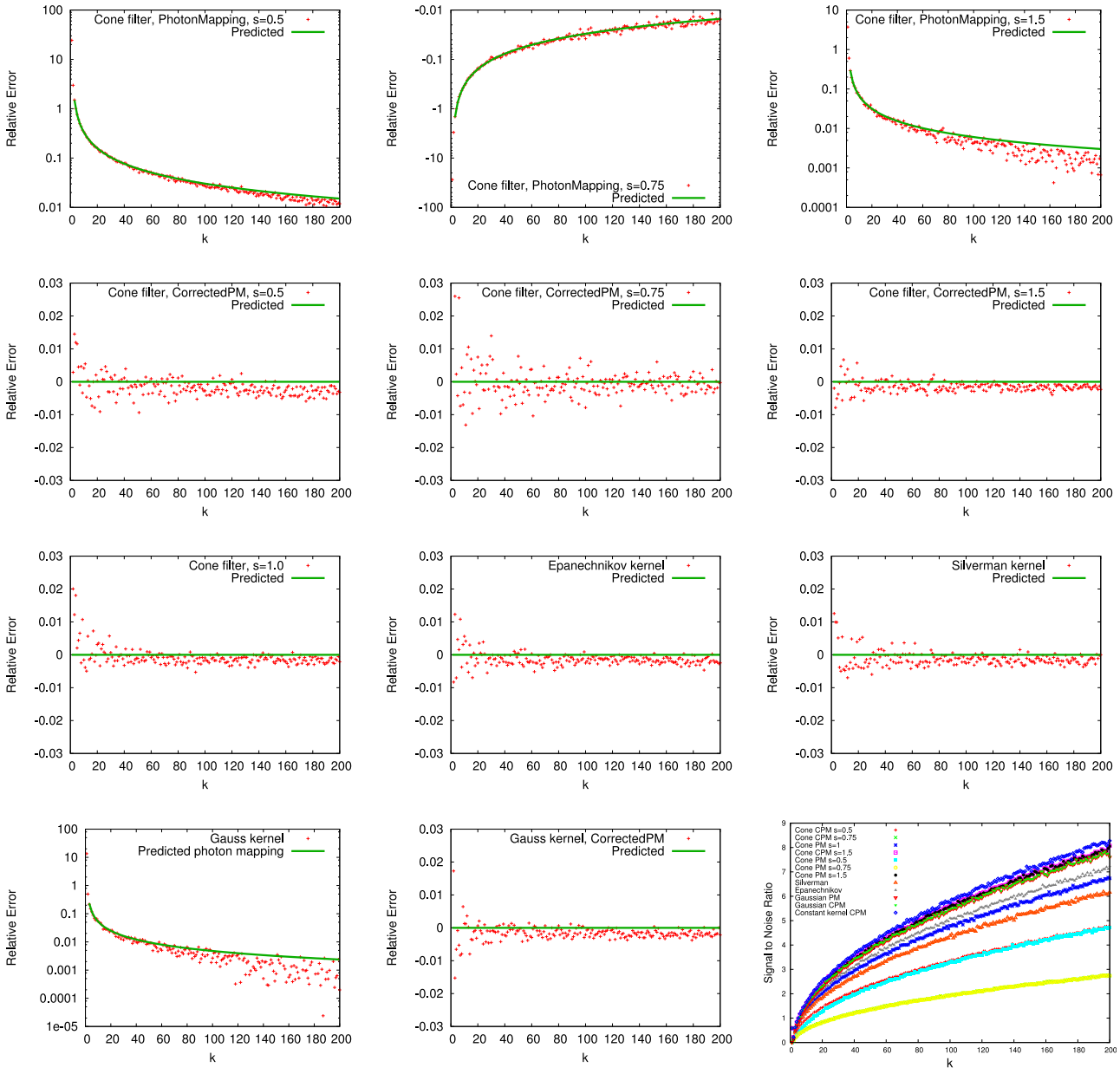

Fig. 5. Relative error of photon mapping (first row, logarithmic plot) and corrected photon mapping (second row, linear plot) with a cone filter using $s = 0.5$ (left), $s = 0.75$ (center), and $s = 1.5$ (right). Third row: Cone filter using $s = 1$ (left), Epanechnikov kernel (center) and Silverman kernel (right). Bottom row: Photon mapping (left) and corrected photon mapping (center) using a Gaussian filter. Right: signal to noise ratio of the different filters. Distribution of photons arising from a point light source, as a function of k (in red); theoretical prediction of the error (in green). The (-1) bias with $k = 1$ for corrected photon mapping is not shown. The boundary bias can be seen as a small underestimation of radiance in all graphs.

Using equation (23):

$$s = 0.5 \quad \rightarrow \frac{(3s-3)I(P)}{(3s-2)(k-1)} = \frac{3}{k-1} I(P) \tag{44}$$

$$s = 0.75 \rightarrow \frac{(3s-3)I(P)}{(3s-2)(k-1)} = -\frac{3}{k-1} I(P) \tag{45}$$

$$s = 1.5 \quad \rightarrow \frac{(3s-3)I(P)}{(3s-2)(k-1)} = \frac{3}{5(k-1)} I(P). \tag{46}$$

Fig. 4 (first row) shows the cases $s = 0.5$, $s = 0.75$ and $s = 1.5$ with the theoretical estimate of the bias, for the original photon maps. The overestimation of radiance can be clearly seen in $s = 0.5$ and $s = 1.5$, and the underestimation is apparent in $s = 0.75$. We can see that the empirical and theoretical solutions agree completely. Fig. 4 (second row) shows our corrected estimate which discards the kth nearest photon, with no bias. Fig. 4 (third row) shows the cone filter with $s = 1$ (left) and the Epanechnikov (center) and Silverman (right) kernels. We can see the absence of bias, as predicted by the theoretical study.

The results for the Gaussian kernel with corrected $\tilde{\alpha}$ can be seen in the fourth row (left and center). We can see the overestimation of the standard estimate (in this case smaller than the estimate using the cone filter, but still noticeable and in good accordance with theoretical predictions) and the absence of bias for our corrected estimate.

Since this scene does not contain any discontinuities in illumination, the results for the specialized differential filter are the same as those of the constant filter ($\tilde{k} = k$). Fig. 4 (bottom right) shows the signal to noise ratio of the different methods. We can see that for a uniform distribution of impacts, the use of kernels is not beneficial, since the increment in variance created by giving more weight to very near photons will not reduce proximity bias, as radiance is constant. Additionally, checking Fig. 1, we see that if we order the kernels by their distance to the constant kernel at the center, this determines the signal to noise ratio ordering as well, except for the Gaussian and cone filter with $s = 1.5$, which have swapped their position.

4.2 Empirical Study of a Point Light Source

To simulate more realistic light conditions, while at the same time being able to calculate analytically the solution, we simulated a scene composed of a disc illuminated by a point light source located above the disc centre.

The fraction of the power which leaves the light source and arrives at the point P in the plane (the form factor) is $\frac{\cos(\theta)}{||P-L||^2}$, with θ denoting the angle between the light vector and the normal, L the light position and P the point of interest. Fig. 3 has a graph of the form factor as a function of the distance to the centre of the disc (the form factor is radially symmetric in this scene).

Fig. 5 (first row) shows the cases $s = 0.5$, $s = 0.75$ and $s = 1.5$ with the theoretical estimate of the bias. We can see again the overestimation of radiance for $s = 0.5$ and $s = 1.5$ and the underestimation in $s = 0.75$. We can see that the empirical and theoretical solutions agree, although proximity bias makes the empirical results underestimate radiance since we are estimating radiance at a maximum. The second row shows our corrected estimate, with no bias.

The third row shows the results for the cone filter with $s = 1$ (left) and the Epanechnikov (center) and Silverman (right) kernels. We can see the slight underestimation of radiance due to the effect of proximity bias, similar to the one present in the corresponding figures from García et al. [3].

The results for the Gaussian kernel with corrected $\tilde{\alpha}$ can be seen in the last row (left and center). We can see the overestimation of the standard estimate and the small proximity bias for our corrected estimate.

Since this scene does not contain any discontinuities in illumination either, the results for the specialized differential filter are again the same as those of the constant filter ($\tilde{k} = k$).

Finally, Fig. 5 (bottom right) shows the signal to noise ratio of the different algorithms. We can see that the signal to noise ratio ordering of the kernels is the same as with a uniform distribution of photons.

5 Conclusions

We have extended the framework presented in García et al. [3] to take into account photon mapping algorithms with general filtering kernels, and provided a theoretical and empirical study of the five most common filtering kernels in the context of photon mapping. The cone filter is consistent when it has slope 1 (meaning weight 0 for the kth nearest impact). For other slopes, discarding photon k is necessary. The 2D Epanechnikov and Silverman kernels are consistent by construction. The Gaussian kernel requires a new normalization constant $\tilde{\alpha} \approx 1.728$ in the case of Photon Maps (otherwise radiance will be underestimated by 46.9 percent), and discarding photon k is also needed. The specialized differential filter is especially affected by the overestimation bias, since it uses a smaller number of photons $\tilde{k} < k$, which translates into a relatively larger bias. Discarding photon $\tilde{k}$ fixes the issue. In summary, we can see that for the six most commonly used kernels (constant, cone filter, Epanechnikov, Silverman, Gaussian and specialized differential filter), four of them are affected by the bias presented in [3], while two are unaffected. The theoretical results have been validated by the empirical study. A study of progressive photon mapping shows that the overestimation bias of the this algorithm's inner photon mapping evaluation is reduced by a factor S, the number of stages in the algorithm. The methodology shown here can be of use to other researchers who want to test the use of other kernels to smooth photon mapping estimates while avoiding new biases.

For future work, we would like to determine the necessary and sufficient properties of the kernel which eliminate the bias studied in this paper. We would also like to study how the use of stratified sampling for photons affects the irradiance estimate. Another line of work is the study of the performance of the different kernels in the general case, with an arbitrary distribution of photons.

Acknowledgments

This work has been supported by the research projects coded TIN2010-21089-C03-01 and IPT-2011-0885-430000 (Spanish Commission for Science and Technology), by Grant 2009SGR643 (Catalan Government), and by FEDER funding from the European Union. The authors would also like to thank all anonymous reviewers for their insightful comments.

References

[1] H. Jensen, "Global illumination using photon maps," in *Proc. Eurograph. Workshop Rendering Tech.*, 1996, pp. 21–30.
[2] M. Wand and C. Jones, *Kernel Smoothing*. Series Monographs on Statistics and Applied Probability, London, U.K. Chapman & Hall, 1995.
[3] R. García, C. Ureña, and M. Sbert, "Description and solution of an unreported intrinsic bias in photon mapping density estimation with constant kernel," *Comput. Graph. Forum*, vol. 31, no. 1, pp. 33–41, 2012.
[4] D. O. Loftsgaarden and C. P. Quesenberry, "A nonparametric estimate of a multivariate density function," *Ann. Math. Statist.*, vol. 36, no. 3, pp. 1049–1051, 1965.
[5] K. Fukunaga, *Introduction to Statistical Pattern Recognition*. 2nd ed. San Diego, CA, USA: Academic, 1990.
[6] T. Hachisuka, S. Ogaki, and H. W. Jensen, "Progressive photon mapping," *ACM Trans. Graph.*, vol. 27, pp. 130:1–130:8, Dec. 2008.
[7] C. Knaus and M. Zwicker, "Progressive photon mapping: A probabilistic approach," *ACM Trans. Graph.*, vol. 30, no. 3, pp. 25:1–25:13, May 2011.
[8] R. García, C. Ureña, and M. Sbert, "Description and solution of an unreported intrinsic bias in photon mapping density estimation with constant kernel," *Presented at Eurographics 24th Symposium on Resdering*. Invited Paper from [3].
[9] A. Wilkie, A. Weidlich, M. Magnor, and A. Chalmers, "Predictive rendering," in *Proc. ACM SIGGRAPH ASIA Courses*, 2009, pp. 1–428.

[10] B. J. Walter, "Density estimation techniques for global illumination," Ph.D. dissertation Ithaca, NY, USA, 1998.
[11] B. Walter, P. M. Hubbard, P. Shirley, and D. P. Greenberg, "Global illumination using local linear density estimation," *ACM Trans. Graph.*, vol. 16, no. 3, pp. 217–259, Jul. 1997.
[12] S. Roland, "Bias compensation for photon maps," *Comput. Graph. Forum*, vol. 22, no. 4, pp. 729–742, 2003.
[13] V. Havran, J. Bittner, and H.-P. Seidel, "Ray maps for global illumination," in *Proc. ACM SIGGRAPH Sketches*, 2004, p. 77.
[14] H. David and H. Nagaraja, *Order Statistics*. New York, NY, USA: Wiley, 2003.
[15] P. Shirley, B. Wade, P. Hubbard, D. Zadeski, B. Walter, and D. Greenberg, "Global illumination via density estimation," in *Proc. Eurograph. Workshop Rendering Tech.*, 1995, pp. 219–230.
[16] H. W. Jensen, "The photon map in global illumination," Ph.D. dissertation, Dept. Graphical Commun., Tech. Univ. Denmark, 1996.
[17] M. J. Pavicic, "Convenient anti-aliasing filters that minimize bumpy sampling," in *Graphics Gems*, A. S. Glassner, Ed., San Diego, CA, USA: Academic, 1990, pp. 144–146.
[18] H. W. Jensen and N. J. Christensen, "A practical guide to global illumination using photon maps," in *Proc. SIGGRAPH*, Course Notes, 2000, pp. 1–78, http: //graphics.stanford.edu/courses/cs348b-00/course8.pdf.
[19] P. Christensen, H. Jensen, and F. Suykens, "A practical guide to global illumination using photon mapping," in *Proc. SIGGRAPH Course Notes*, 2001, pp. 60–90.
[20] E. E. Kummer, "De integralibus quibusdam definitis et seriebus infinitis," *J. für die reine und angewandte Math.*, vol. 1837, no. 17, pp. 228–242, 1837.

Rubén Jesus García Hernández received the PhD degree in the University of Granada, Spain, in 2009. He has been a researcher at the University of Girona since 2010. He has participated in multiple research projects dealing with different aspects of computer graphics and interaction, and has published results in national and international venues. His research interests include realistic image synthesis, videogames, and theoretical studies of algorithms.

Carlos Ureña received the PhD degree in computer science from the University of Granada in 1997, where he currently holds a lecturer position. His research is focused on virtual reality, visualisation and simulation on GPUs, and realistic rendering by using Monte-Carlo sampling algorithms. He has coauthored several journal and conference papers on time-efficient ray-tracing algorithms, on bias analysis and reduction in Photon-mapping systems, on BRDF sampling and on finite-elements based fluid simulation in GPUs. He has collaborated with various companies as a counsellor in computer graphics related projects, and has made reviews for various computer graphics related journals and conferences.

Jordi Poch received the master's of mathematics degree from the Universitat Autnoma de Barcelona in 1983 and the PhD degree in mathematics from the Universitat Politcnica de Catalunya in 1996. He is a lecturer at the Department of Mathematics de la Universitat de Girona. His main research interests include mathematical modeling of adsorption processes in biomaterials and the development and application of new tools to support teaching. He has participated in several national research projects and has been principal investigator of several research projects and improve teaching quality. He has authored and coauthored several articles, both in the area of modeling of adsorption as in the area of e-learning.

Mateu Sbert received the master's degree in physics from the University of Valencia in 1977, the master's degree in mathematics from UNED University in 1984, and the PhD degree in computer science from the Technical University of Catalonia in 1997. Currently, he is a professor of computer science at the University of Girona. His research is mainly focused on the application of Monte Carlo, Integral Geometry, and Information Theory techniques to radiosity, global illumination, image processing, and visualization. He authored or coauthored more than 150 papers in peer reviewed international journals or conferences, two books published by Morgan & Claypool, San Francisco, has participated in many international program committees of international conferences, and been associated editor of two international journals. He received the Best PhD Award.